doi:10.1016/j.jmb.2005.06.080 J. Mol. Biol. (2005) 351, 939–947

JMB

Available online at www.sciencedirect.com

SCIENCE DIRECT®

ELSEVIER

COMMUNICATION

Positioning Membrane Proteins by Novel Protein Engineering and Biophysical Approaches

Suren A. Tatulian[1]*, Shan Qin[1,2], Abhay H. Pande[1] and Xiaomei He[1,3]

[1]*Biomolecular Science Center University of Central Florida 12722 Research Parkway Orlando, FL 32826, USA*

[2]*Department of Molecular Biology, Massachusetts General Hospital, Harvard Medical School, Boston, MA 02114 USA*

[3]*Department of Chemistry University of Central Florida 4000 Central Florida Blvd. Orlando, FL 32816, USA*

**Corresponding author*

Membrane proteins are unique, in that they can function properly only when they are bound to cellular membranes in a distinct manner. Therefore, positioning of membrane proteins with respect to the membrane is required in addition to the three-dimensional structures in order to understand their detailed molecular mechanisms. Atomic-resolution structures of membrane proteins that have been determined to date provide the atom coordinates in arbitrary coordinate systems with no relation to the membrane and therefore provide little or no information on how the protein would interact with the membrane. This is especially true for peripheral membrane proteins, because they, unlike integral proteins, are devoid of well-defined hydrophobic transmembrane domains. Here, we present a novel technique for determination of the configuration of a protein–membrane complex that involves protein ligation, segmental isotope labeling, polarized infrared spectroscopy, membrane depth-dependent fluorescence quenching, and analytical geometry algorithms. We have applied this approach to determine the structure of a membrane-bound phospholipase A_2. Our results provide an unprecedented structure of a membrane-bound protein in which the *z*-coordinate of each atom is the distance from the membrane center and therefore allows precise location of each amino acid relative to the membrane. Given the functional significance of the orientation and location of membrane-bound proteins with respect to the membrane, we propose to specify this structural feature as the "quinary" structure of membrane proteins.

Keywords: membrane protein; orientation; insertion; polarized FTIR; fluorescence quenching

Protein function cannot be understood without knowledge of its structure. For water-soluble proteins, which function in an isotropic aqueous medium, the atomic-resolution structure in most cases provides an ultimate clue to the protein function. Conversely, membrane proteins are destined to operate in a highly anisotropic membrane environment.[1,2] Therefore, even when the atomic structure of a membrane protein is determined, information on the mode of its interaction with the membrane is required in order to understand molecular details of its function.[3–6]

The importance of the angular orientation and the location of the protein relative to the membrane have been well recognized, and several biophysical approaches have been developed to tackle this challenging aspect of membrane protein structure. These include X-ray crystallography of proteins reconstituted in a lipid cubic phase,[2,7] solid-state NMR of peptides or small proteins bound to oriented lipid membranes,[8,9] electron spin resonance of membrane-bound proteins,[10–14] polarized attenuated total reflection Fourier transform infrared (ATR-FTIR) spectroscopy,[15–22] and computational methods.[3,5,23,24]

In spite of the power contained in each of these approaches, they still encounter technical difficulties and are far from becoming routine and straightforward techniques for determination of

Abbreviations used: ATR-FTIR, attenuated total reflection Fourier transform infrared; Br_2PC, 1-palmitoyl-2-stearoyl(dibromo)-*sn*-glycero-3-phosphocholine; PLA_2, phospholipase A_2; POPC, 1-palmitoyl-2-oleoyl-*sn*-glycero-3-phosphocholine; POPG, 1-palmitoyl-2-oleoyl-*sn*-glycero-3-phosphoglycerol.

E-mail address of the corresponding author: statulia@mail.ucf.edu

0022-2836/$ - see front matter

the structure of proteins in biological or artificial lipid membranes. ATR-FTIR spectroscopy has been used to probe the angular orientation of membrane-bound peptides or proteins that possess a rotational/translational symmetry axis, such as single helical peptides,[18–21] β-barrel integral membrane proteins,[22] or protein oligomers with a rotational symmetry axis.[16] The orientation of proteins of irregular shape cannot be achieved easily by this method. In a limited number of cases this has been accomplished, however, by involving protein engineering procedures. For phospholamban, which has a transmembrane and a tilted cytoplasmic helix, the orientations of both helices relative to the membrane normal were determined by measuring the linear infrared dichroic ratios of the truncated transmembrane helix and of the full-length protein.[17] A similar approach was used to assess the orientation of a membrane-bound peripheral protein, human pancreatic phospholipase A_2 (PLA_2), which has an N-terminal and two internal, nearly parallel α-helices.[18] These latter approaches rely heavily on an assumption that the orientation of the truncated fragment of the protein, such as the transmembrane domain of phospholamban or the N-terminal helix of PLA_2, is the same as a separate peptide and as a part of the membrane-bound protein. This is an assumption that may or may not be plausible in the absence of additional experimental evidence.

The orientation of a membrane-bound protein can be obtained in a stringent manner by polarized ATR-FTIR spectroscopy, provided the dichroic ratios of two different helices of the protein are determined. Since all helices in the protein generate a common amide I component, this can be done only if amide I signals from two helices are spectrally dissected, e.g. by isotope labeling. For a multihelix protein this will require labeling of two helices by different isotope combinations, such as one with ^{13}C and the other with both ^{13}C and ^{18}O, whereas for proteins that comprise only two helices, labeling of one helix with ^{13}C will be sufficient to spectrally isolate its amide I signal. In this work, we used this approach to determine the angular orientation of human pancreatic PLA_2, which has three α-helices, helix 1 (residues 1–10), helix 2 (residues 41–57), and helix 3 (residues 91–108). It was possible to apply the two-helix approach to this three-helix protein because helices 2 and 3 are nearly parallel with each other (see below). In addition, the presence of a cysteine residue at position 11, right after the N-terminal α-helix, allowed us to ligate an unlabeled, C-terminally thioesterified N-terminal peptide with a uniformly ^{13}C-labeled C-terminal fragment starting with Cys11. Furthermore, the protein has a single tryptophan residue at position 3, which allows determination of the depth of membrane insertion of Trp3, and consequently of the whole protein molecule, by using membrane depth-dependent fluorescence quenching.

In order to assess the mode of membrane binding of a protein, one needs the structure of the protein. We have obtained the structure of human pancreatic PLA_2 by homology modeling,[25] using the structure of porcine pancreatic PLA_2 as a template (PDB entry 1P2P), which shares 88% sequence identity with its human counterpart. Determination of the orientation of the membrane-bound protein based on the infrared dichroic ratios of α-helices requires the interhelical angles, which were determined as follows. We consider three Cartesian coordinate systems, an "intrinsic" helical coordinate system $\sum_h$ with axes $X_{Hi}Y_{Hi}Z_{Hi}$ assigned to each helix, with Z_{Hi} being the helical axis of the ith helix, the "protein" system $\sum_p$ with axes $X^*Y^*Z^*$, in which the protein atom coordinates are given, and the "membrane" coordinate system $\sum_m$ with axes XYZ that has its XY plane at the membrane center between the two lipid leaflets and the Z axis perpendicular to the membrane surface. The geometry of a right-handed α-helix provides the backbone atom coordinates in the system $\sum_h$: $x_{Hij} = a\cos[100(j-1)]$, $y_{Hij} = a\sin[100(j-1)]$, $z_{Hij} = b(j-1)$, where a is the radius of the helical "cylinder" and b is the height per residue (upper case X, Y, and Z denote the coordinate axes and lower case x, y, and z denote the coordinates). For example, if C^α atoms are considered (C^α atoms are on the surface of the helical cylinder), then for an α-helix $a = 2.25$ Å and $b = 1.5$ Å. Here, the subscript i signifies a certain (ith) helix in the protein molecule and j signifies a certain (jth) amino acid residue in ith helix, moving in an N→C direction. The knowledge of the helical atom coordinates in the helical ($\sum_h$) and the protein ($\sum_p$) systems allows determination of the cosines of angles between the axes of these coordinate systems, $\cos\zeta_{1i}$, $\cos\zeta_{2i}$ and $\cos\zeta_{3i}$, where $\zeta_{1i,2i,3i}$ are the angles (X^*,Z_{Hi}), (Y^*,Z_{Hi}), (Z^*,Z_{Hi}), respectively. The angle θ between the two helical axes (e.g. helices 1 and 2) is then given as:

$$\cos\theta = \frac{A_1A_2 + B_1B_2 + C_1C_2}{\sqrt{(A_1^2 + B_1^2 + C_1^2)(A_2^2 + B_2^2 + C_2^2)}} \quad (1)$$

where:

$$A_i = \frac{1}{\cos\zeta_{2,i}\cos\zeta_{3,i}}, B_i = \frac{1}{\cos\zeta_{1,i}\cos\zeta_{3,i}},$$

$$C_i = \frac{1}{\cos\zeta_{1,i}\cos\zeta_{2,i}}$$

The angle between the helical axes of helices 2 and 3 of PLA_2 was determined through equation (1) to be 173.6°. This allowed us to consider these helices nearly antiparallel to each other and ascribe a common order parameter to them. (In terms of infrared order parameters, parallel and antiparallel orientations are equivalent.) Consequently, the orientation of the membrane-bound protein could be determined using the two-helix approach.

A segmentally ^{13}C-labeled semisynthetic PLA_2 was created in which the N-terminal helix was not

labeled, whereas the rest of the protein was uniformly ^{13}C-labeled. First, the ^{13}C-labeled PLA_2 fragment Cys11–Ser126 was recombinantly expressed in *Escherichia coli* and purified as described,[18] except that uniformly ^{13}C-labeled D-glucose was used in a M9 minimal medium as a sole metabolic source of carbon. The ^{13}C-labeled fragment Cys11–Ser126 was ligated with a C-terminally thioesterified peptide corresponding to the first ten residues of the protein: Ala-Val-Trp-Gln-Phe-Arg-Lys-Met-Ile-Lys-$COSCH_2COOH$, synthesized by SynPep Corp. (Dublin, CA). In thioester to cysteine-type peptide ligation, the thioester functionality reacts with the thiol group of the cysteine side-chain, followed by irreversible S to N acyl transfer and formation of a native peptide bond.[26] Internal cysteine residues, which are abundant in PLA_2, can react with the thioesterified peptide, but these reactions are reversible under appropriately selected reducing conditions and their effect is only to slow the formation of the full-length, segmentally ^{13}C-labeled protein.[27] The segmentally ^{13}C-labeled PLA_2 was refolded and purified to homogeneity using ion-exchange and size-exclusion chromatography (Figure 1(a) and (b)). The protein was shown to be the full-length PLA_2 by immunoblotting, as it reacted with antibodies raised against both the N-terminal peptide and the Cys11–Ser126 fragment (Figure 1(c)). The specific activity of the semisynthetic protein was similar to that of the recombinant PLA_2 (Figure 1(d)).

Isotope-labeling of helices 2 and 3 resulted in a splitting of the infrared amide I signal of the membrane-bound protein. The unlabeled helix 1 generated an amide I component at 1656 cm^{-1}, whereas the amide I component of the ^{13}C-labeled helices 2 and 3 was shifted to 1616 cm^{-1} (Figure 2(a) and (b)). Spectrally separated amide I signals of the unlabeled helix 1 and the ^{13}C-labeled helices 2 and 3 at parallel and perpendicular polarizations of the infrared light were used to determine the respective order parameters, as described.[15,18] The order parameter of helix 1 was -0.142, and that of helices 2 and 3 was -0.405. This allowed determination of the cosines of angles between the helical axes and the membrane normal, $\cos(ZZ_{H1}) = \pm 0.489$ and $\cos(ZZ_{H2}) = \pm 0.252$, where Z_{H1} and Z_{H2} are the helical axis of helix 1 and an axis describing the orientation of helices 2 and 3. Because of the rotational freedom of the protein about the membrane normal (Z-axis), the plus and minus signs of the cosines are equivalent. Orientations of helices in the membrane system $\sum_m$, i.e. $\cos(ZZ_{H1})$ and $\cos(ZZ_{H2})$, were expressed through orientations of helices in the protein coordinate system

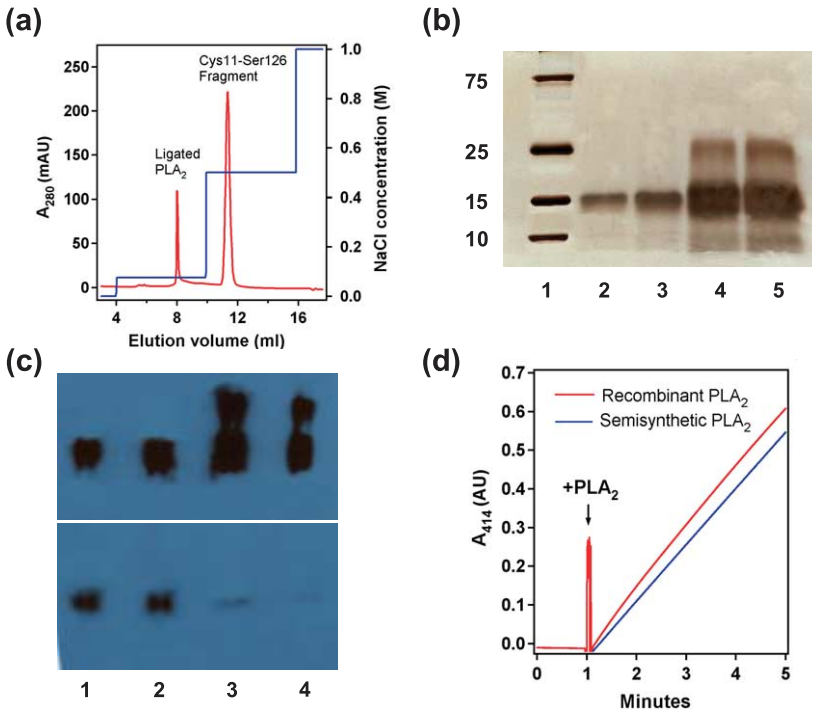

Figure 1. Purification and characterization of the semisynthetic, segmentally ^{13}C-labeled human pancreatic PLA_2. The ^{13}C-labeled fragment Cys11–Ser126 was reacted with a C-terminally thioesterified decapeptide in a buffer containing 6 M guanidinum-HCl, 100 mM sodium phosphate (pH 7.4), 5% (v/v) β-mercaptoethanol, 1 mM EDTA, 4% (v/v) thiophenol, and 4% (v/v) benzyl mercaptan. The reaction was allowed to proceed for six hours at 37 °C, followed by refolding of the ligated protein and purification using ion-exchange Mono Q 5/50 and size-exclusion HiLoad Superdex-75 column chromatography, as described.[18] PLA_2 activity was measured using diheptanoyl-thio-phosphatidylcholine as a substrate, as described.[18] (a) Profile of elution of the sample from the Mono Q column (red, left axis) with a stepwise increase in the concentration of NaCl (blue, right axis). (b) Silver-stained SDS/polyacrylamide gel of the elution fractions corresponding to the ligated product (lanes 2 and 3) and the free Cys11–Ser126 fragment (lanes 4 and 5). Lane 1 shows the molecular mass markers. (c) A Western blot of the ligated PLA_2 (lanes 1 and 2) and the free Cys11–Ser126 fragment (lanes 3 and 4) using mouse anti-Cys11–Ser126 as a primary antibody and anti-mouse horseradish peroxidase as a secondary antibody (top), and using mouse-anti-Ala1–Lys10 as primary antibody and the same secondary antibody (bottom). The pure semisynthetic, segmentally ^{13}C-labeled PLA_2 reacted with both antibodies raised against the Cys11–Ser126 fragment and the N-terminal peptide. (d) Lipid hydrolysis assays indicated that the activity of the semisynthetic, segmentally ^{13}C-labeled PLA_2 (blue) was similar to that of the recombinant PLA_2 (red).

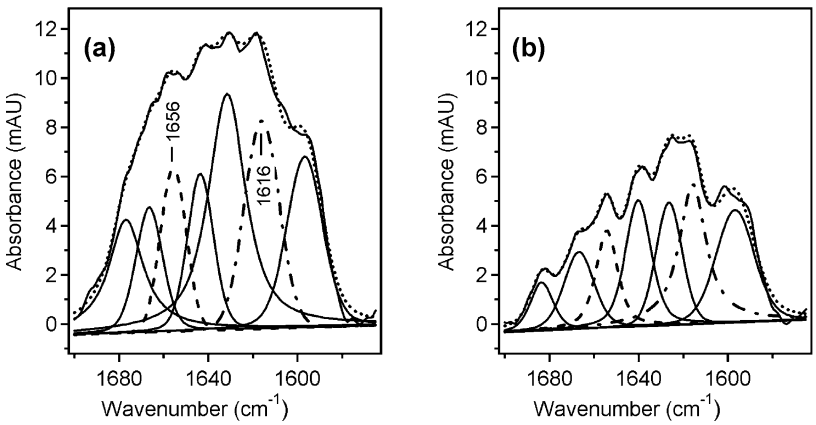

Figure 2. Determination of the angular orientation of PLA_2 by polarized ATR-FTIR spectroscopy. The phospholipid bilayer, supported on a germanium internal reflection plate, was composed of 80 mol% 1-palmitoyl-2-oleoyl-*sn*-glycero-3-phosphocholine (POPC) and 20 mol% 1-palmitoyl-2-oleoyl-*sn*-glycero-3-phosphoglycerol (POPG). The semisynthetic, segmentally ^{13}C-labeled PLA_2 was dissolved in a ^2H_2O-based buffer containing 100 mM NaCl, 1 mM NaN_3, 1 mM EGTA, 50 mM Hepes (pD 7.4) and injected into the cell containing the supported membrane, which was followed by measurements of ATR-FTIR spectra at (a) parallel and (b) perpendicular polarizations of the infrared light. Amide I components were generated by curve-fitting, as described.[18] The components corresponding to the N-terminal unlabeled α-helix (broken line) and the two ^{13}C-labeled α-helices (dash-dot line) are centered at 1656 cm^{-1} and at 1616 cm^{-1}. The ratio of their intensities is significantly higher than the ratio of relative numbers of amino acid residues in the respective helices, because of higher extinction coefficient of ^{12}C-helical *versus* ^{13}C-helical segments.[45] The sum of all components is shown by the dotted line.

$\sum_p$ and the cosines of angles between the coordinate systems $\sum_p$ and $\sum_m$:

$$\cos(ZZ_{H1}) = l_3u_{11} + m_3u_{21} + n_3u_{31} \quad (2)$$

and:

$$\cos(ZZ_{H2}) = l_3u_{12} + m_3u_{22} + n_3u_{32} \quad (3)$$

where $l_3=\cos(Z,X^*)$, $m_3=\cos(Z,Y^*)$, $n_3=\cos(Z,Z^*)$, $u_{1,i}=\cos(X^*,Z_{Hi})$, $u_{2,i}=\cos(Y^*,Z_{Hi})$, $u_{3,i}=\cos(Z^*,Z_{Hi})$. All values of u_{ij}, i.e. the orientations of all helices relative to the axes of the protein coordinate system $\sum_p$, were determined using the C^α atom coordinates of the protein, based on an algorithm developed in this laboratory. Equations (2) and (3) then contain three unknowns: l_3, m_3, and n_3, i.e. a third equation is needed to find these cosines. The third equation is simply given by the law of direction cosines: $l_3^2 + m_3^2 + n_3^2 = 1$. The three equations were solved together and the values of cosines of the angles between the three axes of the protein coordinate system $\sum_p$ and the membrane normal were determined as $l_3 = -0.301$, $m_3 = -0.256$, $n_3 = 0.919$.

Our task is to obtain the coordinates of the membrane-bound protein in the membrane coordinate system $\sum_m$. In order to do this, the other six cosines, i.e. those of the angles between the *X* and *Y* axes, and the axes *X**, *Y**, and *Z**, were needed in addition to l_3, m_3, and n_3. Because of the rotational freedom of the membrane-bound protein about the *Z*-axis, all azimuthal angles (determined by rotation about the *Z* axis) are equally valid. Therefore, without the loss of generality, one of the six cosines was selected arbitrarily (e.g. $\cos(Y,X^*) = 0.456$), and the other five cosines were found using the laws of direction cosines. This yielded $l_1 \equiv \cos(X, X^*) = -0.837$, $l_2 \equiv \cos(Y,X^*) = 0.456$, $m_1 \equiv \cos(X,Y^*) = 0.532$, $m_2 \equiv \cos(Y,Y^*) = 0.807$, $n_1 \equiv \cos(X,Z^*) = -0.127$, $n_2 \equiv \cos(Y,Z^*) = 0.374$. The nine direction cosines between the membrane and protein coordinate systems, which were considered to be translationally co-centered, were used to transfer the protein atom coordinates from the protein system $\sum_p(x_i^*, y_i^*, z_i^*)$ to the membrane system $\sum_m$ (x_i, y_i, z_i):

$$\left.\begin{aligned} x_i &= l_1x_i^* + m_1y_i^* + n_1z_i^* \\ y_i &= l_2x_i^* + m_2y_i^* + n_2z_i^* \\ z_i &= l_3x_i^* + m_3y_i^* + n_3z_i^* \end{aligned}\right\} \quad (4)$$

These coordinates present the structure of the membrane-bound protein with an angular orientation corresponding to the mode of membrane binding, but do not specify the translational location of the protein relative to the membrane normal (coordinate transformation was done, assuming that the systems $\sum_m$ and $\sum_p$ have a common origin).

In order to locate the protein in the vertical dimension (the membrane normal *Z*-axis), we have measured membrane depth-dependent quenching of the single tryptophan residue (Trp3) of PLA_2. Membrane depth-dependent fluorescence quenching by vesicles containing 1-palmitoyl-2-stearoyl-(dibromo)-*sn*-glycero-3-phosphocholines (Br_2PC) brominated at the 6,7, or 9,10, or 11,12 positions of acyl chains indicated that Trp3 of the membrane-bound protein was quenched maximally by 9,10-Br_2PC (Figure 3). The distribution analysis of Trp3 fluorescence quenching[28] indicated that Trp3 was located at 9.0(±1) Å from the membrane center (Figure 3, inset). Experiments with membranes containing 20 mol% or 40 mol% anionic lipid yielded similar results. Significant insertion of tryptophan into the membrane hydrocarbon region is consistent with NMR experiments indicating that indole induced a maximum chemical shift of POPC at the level of the acyl chain C3 carbon atoms

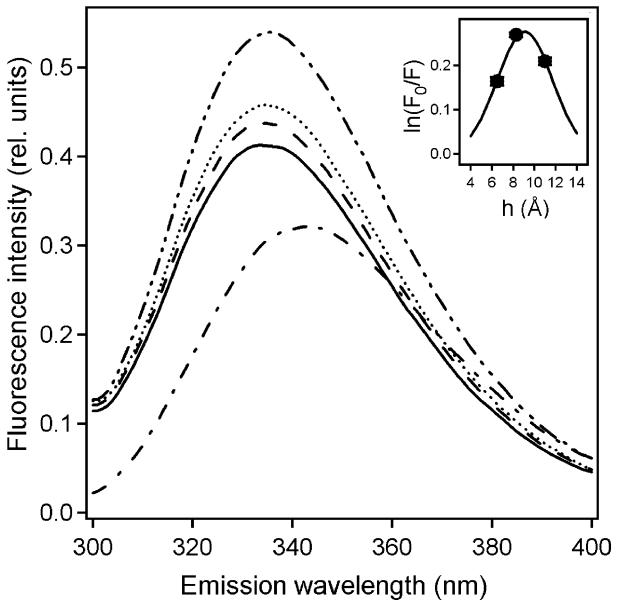

Figure 3. Determination of the depth of membrane insertion of PLA_2 by fluorescence quenching experiments. Fluorescence experiments were conducted at 25 °C, as described.[18] The protein and lipid (if present) concentrations were 4 μM and 0.5 mM, respectively. Large unilamellar lipid vesicles were prepared in a buffer of 10 mM Hepes (pH 7.0), 1 mM EGTA by vortex mixing and extruding through two stacked 100 nm pore-size polycarbonate membranes using a Liposofast extruder (Avestin, Ottawa, Canada). The excitation wavelength was 290 nm. In quenching experiments, vesicles contained 25 mol% Br_2PC. The rest was either 35 mol% POPC and 40 mol% POPG or 55 mol% POPC and 20 mol% POPG, which yielded similar results in terms of tryptophan insertion into the membrane. Fluorescence spectra of recombinant PLA_2 in buffer (dash-dot line), in the presence of POPC/POPG (3:2 molar ratio) vesicles (dash-double-dot line), and vesicles containing Br_2PCs brominated at 6,7 (dotted line), or 9,10 (continuous line), or 11,12 (broken line) positions. The inset shows the distribution analysis of Trp fluorescence quenching by Br_2PCs.

located at 11–12 Å from the membrane center.[29] Jain and Maliwal have shown significant quenching of Trp3 of porcine pancreatic PLA_2 by brominated lipids and fatty acids in sonicated vesicles composed of phosphatidylcholine, lysophosphatidylcholine, and fatty acid.[30] The quenching efficiency was maximal with the fatty acid brominated at the 11,12-position, and decreased when bromine groups were closer to the carboxyl group. These data would indicate significant insertion of PLA_2 into the vesicle membranes, but reaching such a conclusion was prevented by the fact that quenching of Trp3 fluorescence by water-soluble succinimide was suppressed only slightly upon membrane binding of PLA_2. However, later findings showed that the fluorescence of Trp3 of PLA_2 bound to anionic membranes could not be affected by either water-soluble quenchers (acrylamide or succinimide) or even by deuterated water.[31] Also, binding of PLA_2 to micelles of hexadecyl-propanediol-phosphocholine resulted in substantial (>15-fold) decrease in the accessibility of succinimide to Trp3.[32] These findings, together with preferential quenching of Trp3 by bromine at the C9-C11 positions of lipids or fatty acids[30] are consistent with insertion of Trp3 half-way to the membrane center. Furthermore, Jain and Vaz have measured the efficiency of energy transfer between Trp3 of membrane-bound porcine pancreatic PLA_2 and the dansyl chromophore attached to the headgroup of hexadecyl-phosphorylethanolamine in anionic membranes to be $E > 0.95$, which was used to estimate a distance between Trp3 and the membrane surface $r \approx 8$ Å using a Förster distance of $R_o = 17$–18 Å for the Trp-dansyl pair.[31] Using $E = 0.96$ and $R_o = 17.5$ Å, we obtain $r \approx 10.3$ Å, using the equation:

$$r^6 = (1 - E)R_0^6/E$$

Using a more recently reported value of $R_o = 22.5$ Å,[33] one obtains $r \approx 13.2$ Å. Because Trp3 of a membrane-bound PLA_2 cannot be located >10 Å above the membrane surface, the only choice is to locate Trp3 10–13 Å below the membrane surface, i.e. approximately 9 Å from the membrane center, which is in good agreement with our data.

On the basis of our results on quenching of Trp3 by brominated lipids, the *z*-coordinates of all protein atoms were translationally modified so the *z*-coordinate of the geometric center of the indole ring of Trp3 was 9 Å. Thus, the combination of homology modeling, polarized ATR-FTIR, and fluorescence quenching experiments yielded the atomic structure of the membrane-bound PLA_2 with precise angular orientation and the depth of membrane insertion.

The final steps of construction of the structure of the membrane-bound PLA_2 involved adjustment of side-chain conformations of several residues. This procedure is justified, because the homology modeling did not consider protein–membrane interactions, which are likely to cause reorientation of certain side-chains involved in intimate contact with the membrane.[1,3,5,6] The coordinates of the side-chain of Trp3 were modified so the indole ring was in the *XZ* plane, because both NMR data and molecular dynamics simulations indicated an orientation of the tryptophan indole ring parallel with the membrane normal.[24,29] The resulting geometric center of the Trp3 indole ring was placed at 9 Å from the membrane center. Finally, the side-chains of Arg6, Lys10, and Asp17 were reoriented so their ionizable groups were not embedded into the hydrocarbon interior of the membrane. The final model of membrane-bound PLA_2 is presented in Figure 4.

Apart from the protein molecule, Figure 4 shows three planes of atoms that are perpendicular to the membrane normal and are introduced merely to identify the locations of terminal methyl carbon

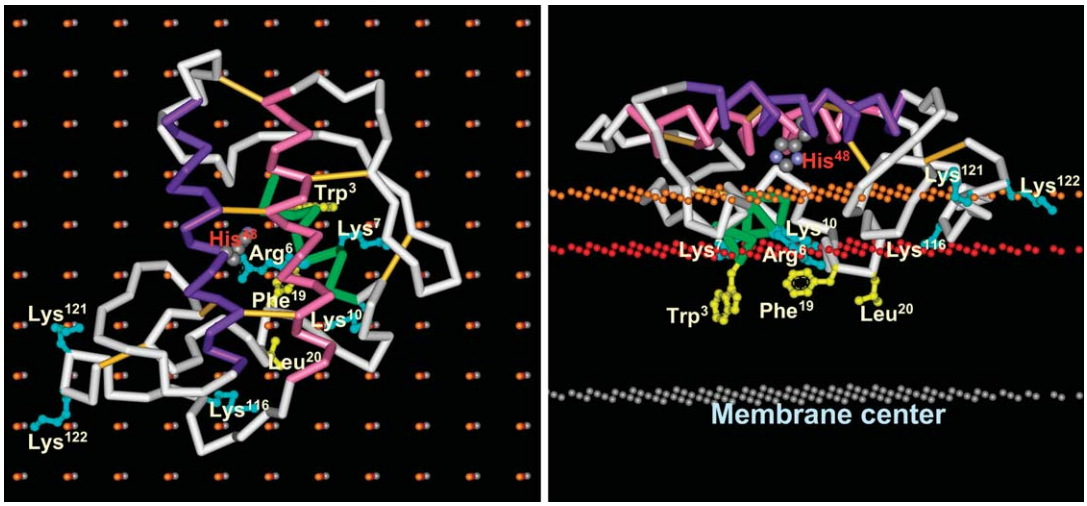

Figure 4. Top (left) and side (right) views of human pancreatic PLA_2 bound to a phospholipid membrane. The structure of PLA_2 was homology-modeled by SWISS-MODEL using porcine pancreatic PLA_2 structure (PDB entry 1P2P) as a template. The protein is shown in a C^{α} stick format, with the α-helices 1, 2, and 3 colored green, purple, and pink, respectively. The side-chains of amino acid residues involved directly in physical interactions with the membrane are shown in ball-and-stick format, hydrophobic residues in yellow and the cationic residues in light blue. The catalytic His48 is shown in CPK format and colored according to the atom type. The three layers of non-protein atoms are introduced to show schematically membrane sections corresponding to the acyl chain terminal methyl carbon atoms (gray), the *sn*-1 carbonyl oxygen atoms (red), and the phosphorus atoms (orange) of membrane glycerophospholipids. In the left panel, the whole structure is rotated slightly about the *Y*-axis in order to show the carbonyl oxygen atoms and the terminal methyl carbon atoms behind the phosphorus atoms of the lipids. Without this rotation, the plane of the picture would coincide with the *XY* plane, and the *Z*-axis would run straight toward the viewer. In the right panel, the structure is rotated by 90° about the *X*-axis, by 120° about the *Z*-axis, and then slightly (<5°) about the resulting horizontal axis in order to show the "3D" planes of lipid "atoms". In this view, the substrate-binding pocket of PLA_2 is turned toward the viewer with a tilt against the membrane surface.

atoms of the acyl chains of glycerophospholipids (membrane center), the *sn*-1 carbonyl oxygen atoms, and the phosphorus atoms of lipid phosphate groups. The *z*-coordinates of these three planes are $z=0$, $z=14.5$ Å, and $z=20$ Å, respectively, which is based on X-ray diffraction data,[34] showing that the "hydrophobic thickness" of POPC bilayers (i.e. the spacing between the *sn*-1 carbonyl oxygen atoms) was 29 Å, and the spacing between the headgroup electron density peaks was 40 Å. This is consistent with the average hydrophobic thickness (29 Å) of a variety of membranes containing integral proteins.[6] The model shown in Figure 4 presents an unprecedented case of positioning a membrane-bound protein in a coordinate system attached to the membrane so that the *z*-coordinate of each protein atom is its distance from the membrane center. This structure identifies explicitly the geometric configuration of the protein–membrane complex, and provides the precise location of each amino acid residue of the protein with respect to the membrane.

The molecular mechanism of a membrane protein can be understood only when the mode of its interaction with the membrane is determined in addition to its atomic structure. This was very well formulated by Basyn *et al.*, who stated: "Few structures of membrane proteins are known and their relationships with the membrane are unclear."[5] In other words, determination of the atomic structure is not the final step in structural characterization of a membrane protein simply because the membrane protein cannot be considered separate from the membrane, and in order to consider it within the context of the membrane, the explicit, experimentally determined mode of its interaction with the membrane is required. In fact, there are numerous lines of evidence showing that the geometric relationship of a membrane protein with the membrane is crucial for the membrane protein function. For example, the pore-forming capabilities of membrane-bound antibiotic peptides are determined by their specific angular orientation with respect to the membrane plane.[21] Transitions between the open and closed states of certain ion channels are mediated by changes in the tilt angles of helices with respect to the membrane normal,[35–37] leading to a "gating-by-tilt" mechanism.[38] Sarcoplasmic reticulum Ca^{2+}-ATPase switches from the Ca^{2+}-bound to the Ca^{2+}-free state by rotational and translational movements of the transmembrane helices relative to the membrane normal, resulting in Ca^{2+} release.[39] Influenza hemagglutinin induces membrane fusion at acidic pH by undergoing an acid-induced inclination toward the membrane surface.[16] Significant changes in the catalytic activity of membrane-bound human group IIA PLA_2 upon variation of the membrane surface charge have been interpreted in terms of a subtle (~15°) change in the angular

orientation of PLA_2 relative to the membrane plane.[12,40] Clearly, the knowledge of the primary, secondary, tertiary, and quaternary structures of membrane proteins is not enough to completely understand their mechanisms. The utmost functional importance of the configuration of protein–membrane complexes warrants consideration of a new, fifth level of membrane protein structure; namely, the "quinary" structure, which signifies the rotational and translational positioning of a membrane protein with respect to the membrane.

The quinary structure of a membrane protein with known atomic-resolution structure provides significant information on the protein mechanism. The model shown in Figure 4 shows clearly that the membrane binding of PLA_2 is stabilized by hydrophobic, ionic, and hydrogen bonding interactions. The side-chains of Trp3, Phe19, and Leu20 act as hydrophobic anchors in membrane docking of PLA_2. Six cationic residues that support membrane binding of PLA_2 are divided into two groups; four of them (Arg6, Lys7, Lys10, and Lys116) are ideally located for hydrogen-bonding with the lipid carbonyl oxygen atoms, while the side-chain amino groups of Lys121 and Lys122 are at the level of lipid phosphate groups, and are most likely involved in ionic interactions with lipid headgroups. This feature may explain earlier puzzling data showing an increase in the membrane-binding affinity of bee venom PLA_2 incorporating five Lys to Glu mutations with increasing fraction of anionic lipid in membranes.[41] If hydrogen bonding interactions are more important than ionic interactions, as suggested by our model (Figure 4), then replacement of Arg or Lys residues of PLA_2 by Glu may result in protonation of the Glu carboxyl groups due to local low pH at the surface of anionic membranes, followed by COOH···O=C hydrogen bonding with ester carbonyl oxygen atoms of lipids. The helices 2 and 3 of PLA_2 are nearly parallel with the membrane plane, and the entrance to the substrate-binding pocket is turned toward the membrane surface with a slight tilt, consistent with previous assessments of the membrane-binding mode of group I/II secretory PLA2s.[12,18,42–44] Because in the model presented in Figure 4 the z-coordinates of protein atoms are the distances from the membrane center, the structure allows easy quantitative inspection of the location of any amino acid residue of interest from the lipid structural groups, which provides insight into the molecular details of the enzyme function. For example, although it is not well understood how the phospholipid molecule penetrates into the substrate-binding pocket of the enzyme, the substrate is thought to travel ~15 Å to reach the catalytic residues.[43,44] In the model in Figure 4, the imidazole nitrogen atoms of catalytic His48 are at 23.5 Å from the membrane center, i.e. the distance between the *sn*-2 ester group and the catalytic site is only ~7 Å. Appreciable insertion of PLA_2 into the membrane implies that, in order to reach the catalytic site, the phospholipid substrate has to travel a much shorter distance than thought earlier. This evidently facilitates a productive interaction between the phospholipid substrate and the membrane-bound enzyme.

In conclusion, this study presents a powerful experimental/computational tool for determination of the positioning of proteins with respect to membranes. This technique yields the structure of the protein–membrane complex at the highest possible level of precision, i.e. the protein structure in an intrinsic coordinate system of the membrane, where the z-coordinate of each protein atom is the distance from the membrane center. This approach is likely to become a fundamental tool for determination and analysis of the quinary structure of membrane proteins, which will undoubtedly provide valuable information on the molecular mechanisms of this important class of proteins.

Protein Data Bank accession number

The coordinates of the membrane-bound PLA_2, where the z-coordinates of the protein atoms are their distances from the membrane center, have been deposited in the Protein Data Bank (accession code 1YSK).

Acknowledgements

We thank J. Lakowicz, A. S. Ladokhin, and T. L. Selby for useful comments during the writing of the manuscript. This work was supported by NIH grant HL65524.

References

1. Chamberlain, A. K. & Bowie, J. U. (2004). Analysis of side-chain rotamers in transmembrane proteins. *Biophys. J.* **87**, 3460–3469.
2. Cartailler, J.-P. & Luecke, H. (2003). X-ray crystallographic analysis of lipid–protein interactions in the bacteriorhodopsin purple membrane. *Annu. Rev. Biophys. Biomol. Struct.* **32**, 285–310.
3. Basyn, F., Charloteaux, B., Thomas, A. & Brasseur, R. (2001). Prediction of membrane protein orientation in lipid bilayers: a theoretical approach. *J. Mol. Graph. Model.* **20**, 235–244.
4. White, S. H., Ladokhin, A. S., Jayasinghe, S. & Hristova, K. (2001). How membranes shape protein structure. *J. Biol. Chem.* **276**, 32395–32398.
5. Basyn, F., Spies, B., Bouffioux, O., Thomas, A. & Brasseur, R. (2003). Insertion of X-ray structures of proteins in membranes. *J. Mol. Graph. Model.* **22**, 11–21.
6. Lee, A. G. (2003). Lipid–protein interactions in biological membranes: a structural perspective. *Biochim. Biophys. Acta*, **1612**, 1–40.
7. Landau, E. M., Pebay-Peyroula, E. & Neutze, R. (2003). Structural and mechanistic insight from high resolution structures of archaeal rhodopsins. *FEBS Letters*, **555**, 51–56.

8. Nevzorov, A. A., Mesleh, M. F. & Opella, S. J. (2004). Structure determination of aligned samples of membrane proteins by NMR spectroscopy. *Magn. Reson. Chem.* **42**, 162–171.
9. Bechinger, B., Aisenbrey, C. & Bertani, P. (2004). The alignment, structure and dynamics of membrane-associated polypeptides by solid-state NMR spectroscopy. *Biochim. Biophys. Acta*, **1666**, 190–204.
10. Malmberg, N. J. & Falke, J. J. (2005). Use of EPR power saturation to analyze the membrane-docking geometries of peripheral proteins: applications to C2 domains. *Annu. Rev. Biophys. Biomol. Struct.* **34**, 71–90.
11. Lin, Y., Nielsen, R., Murray, D., Hubbell, W. L., Mailer, C., Robinson, B. H. & Gelb, M. H. (1998). Docking phospholipase A_2 on membranes using potential-modulated spin relaxation magnetic resonance. *Science*, **279**, 1925–1929.
12. Canaan, S., Nielsen, R., Ghomashchi, F., Robinson, B. H. & Gelb, M. H. (2002). Unusual mode of binding of human group IIA secreted phospholipase A_2 to anionic interfaces as studied by continuous wave and time domain electron paramagnetic resonance spectroscopy. *J. Biol. Chem.* **277**, 30984–30990.
13. Ball, A., Nielsen, R., Gelb, M. H. & Robinson, B. H. (1999). Interfacial membrane docking of cytosolic phospholipase A_2 C2 domain using electrostatic potential-modulated spin relaxation magnetic resonance. *Proc. Natl Acad. Sci. USA*, **96**, 6637–6642.
14. Rufener, E., Frazier, A. A., Wieser, C. M., Hinderliter, A. & Cafiso, D. S. (2005). Membrane-bound orientation and position of the synaptotagmin C2B domain determined by site-directed spin labeling. *Biochemistry*, **44**, 18–28.
15. Tatulian, S. A. (2003). Attenuated total reflection Fourier transform infrared spectroscopy: a method of choice for studying membrane proteins and lipids. *Biochemistry*, **42**, 11898–11907.
16. Tatulian, S. A., Hinterdorfer, P., Baber, G. & Tamm, L. K. (1995). Influenza hemagglutinin assumes a tilted conformation during membrane fusion as determined by attenuated total reflection FTIR spectroscopy. *EMBO J.* **14**, 5514–5523.
17. Tatulian, S. A., Jones, L. R., Reddy, L. G., Stokes, D. L. & Tamm, L. K. (1995). Secondary structure and orientation of phospholamban reconstituted in supported bilayers from polarized attenuated total reflection FTIR spectroscopy. *Biochemistry*, **34**, 4448–4456.
18. Qin, S., Pande, A. H., Nemec, K. N. & Tatulian, S. A. (2004). The N-terminal α-helix of pancreatic phospholipase A_2 determines productive-mode orientation of the enzyme at the membrane surface. *J. Mol. Biol.* **344**, 71–89.
19. Tucker, M. J., Getahun, Z., Nanda, V., DeGrado, W. F. & Gai, F. (2004). A new method for determining the local environment and orientation of individual side chains of membrane-binding peptides. *J. Am. Chem. Soc.* **126**, 5078–5079.
20. Kóta, Z., Páli, T. & Marsh, D. (2004). Orientation and lipid-peptide interactions of gramicidin A in lipid membranes: polarized attenuated total reflection infrared spectroscopy and spin-label electron spin resonance. *Biophys. J.* **86**, 1521–1531.
21. Chia, C. S. B., Torres, J., Cooper, M. A., Arkin, I. T. & Bowie, J. H. (2002). The orientation of the peptide maculatin 1.1 in DMPG and DMPC lipid bilayers. Support for a pore-forming mechanism. *FEBS Letters*, **512**, 47–51.
22. Marsh, D. (2000). Infrared dichroism of twisted β-sheet barrels. The structure of *E. coli* outer membrane proteins. *J. Mol. Biol.* **297**, 803–808.
23. Ash, W. L., Zlomislic, M. R., Oloo, E. O. & Tieleman, D. P. (2004). Computer simulations of membrane proteins. *Biochim. Biophys. Acta*, **1666**, 158–189.
24. Berneche, S., Nina, M. & Roux, B. (2003). Molecular dynamics simulation of melittin in a dimyristoylphosphatidylcholine bilayer membrane. *Biophys. J.* **75**, 1603–1618.
25. Schwede, T., Kopp, J., Guex, N. & Peitsch, M. C. (2003). SWISS-MODEL: an automated protein homology-modeling server. *Nucl. Acids Res.* **31**, 3381–3385.
26. Tam, J. P., Yu, Q. & Miao, Z. (1999). Orthogonal ligation strategies for peptide and protein. *Biopolymers*, **51**, 311–332.
27. Hackeng, T. M., Mounier, C. M., Bon, C., Dawson, P. E., Griffen, J. H. & Kent, S. B. H. (1997). Total chemical synthesis of enzymatically active human type II secretory phospholipase A_2. *Proc. Natl Acad. Sci. USA*, **94**, 7845–7850.
28. London, E. & Ladokhin, A. S. (2002). Measuring the depth of amino acid residues in membrane-inserted peptides by fluorescence quenching. *Curr. Top. Membr.* **52**, 89–115.
29. Yau, W. M., Wimley, W. C., Gawrisch, K. & White, S. H. (1998). The preference of tryptophan for membrane interfaces. *Biochemistry*, **37**, 14713–14718.
30. Jain, M. K. & Maliwal, B. P. (1985). The environment of tryptophan in pig pancreatic phospholipase A2 bound to bilayers. *Biochim. Biophys. Acta*, **814**, 135–140.
31. Jain, M. K. & Vaz, W. L. C. (1987). Dehydration of the lipid-protein microinterface on binding of phospholipase A_2 to lipid bilayers. *Biochim. Biophys. Acta*, **905**, 1–8.
32. Jain, M. K. & Maliwal, B. P. (1993). Spectroscopic properties of the states of pig pancreatic phospholipase A_2 at interfaces and their possible molecular origin. *Biochemistry*, **32**, 11838–11846.
33. Lakowicz, J. R. (1999). *Principles of Fluorescence Spectroscopy* (2nd edit.), Kluwer Academic/Plenum Publishers, New York.
34. McIntosh, T. J. & Holloway, P. W. (1987). Determination of the depth of bromine atoms in bilayers formed from bromolipid probes. *Biochemistry*, **26**, 1783–1788.
35. Edwards, M. D., Li, Y., Kim, S., Miller, S., Bartlett, W., Black, S. *et al*. (2005). Pivotal role of the glycine-rich TM3 helix in gating the MscS mechanosensitive channel. *Nature Struct. Mol. Biol.* **12**, 113–119.
36. Perozo, E., Cortes, D. M., Sompornpisut, P., Kloda, A. & Martinac, B. (2002). Open channel structure of MscL and the gating mechanism of mechanosensitive channels. *Nature*, **418**, 942–948.
37. Sukharev, S., Durell, S. R. & Guy, H. R. (2001). Structural models of the MscL gating mechanism. *Biophys. J.* **81**, 917–936.
38. Turner, M. S. & Sens, P. (2004). Gating-by-tilt of mechanically sensitive membrane channels. *Phys. Rev. Letters*, **93**, 118103.
39. Toyoshima, C. & Nomura, H. (2002). Structural changes in the calcium pump accompanying the dissociation of calcium. *Nature*, **418**, 605–611.
40. Beers, S. A., Buckland, A. G., Giles, N., Gelb, M. H. & Wilton, D. C. (2003). Effect of tryptophan insertions on the properties of the human group IIA phospholipase A_2: mutagenesis produces an enzyme with characteristics similar to those of the human group V phospholipase A_2. *Biochemistry*, **42**, 7326–7338.

41. Bollinger, J. G., Diraviyam, K., Ghomashchi, F., Murray, D. & Gelb, M. H. (2004). Interfacial binding of bee venom secreted phospholipase A_2 to membranes occurs predominantly by a nonelectrostatic mechanism. *Biochemistry*, **43**, 13293–13304.
42. Liu, X., Zhu, H., Huang, B., Rogers, J., Yu, B.-Z., Kumar, A. *et al*. (1995). Phospholipase A_2 engineering. Probing the structural and functional roles of N-terminal residues with site-directed mutagenesis, X-ray, and NMR. *Biochemistry*, **34**, 7322–7334.
43. Yu, B. Z., Janssen, M. J. W., Verheij, H. M. & Jain, M. K. (2000). Control of the chemical step by leucine-31 of pancreatic phospholipase A_2. *Biochemistry*, **39**, 5702–5711.
44. Berg, O. G., Gelb, M. H., Tsai, M. D. & Jain, M. K. (2001). Interfacial enzymology: the secreted phospholipase A_2-paradigm. *Chem. Rev.* **101**, 2613–2654.
45. Venyaminov, S. Y., Hedstrom, J. F. & Prendergast, F. G. (2001). Analysis of the segmental stability of helical peptides by isotope-edited infrared spectroscopy. *Proteins: Struct. Funct. Genet.* **45**, 81–89.

Edited by G. von Heijne

(Received 12 May 2005; received in revised form 7 June 2005; accepted 30 June 2005)
Available online 18 July 2005